J Incl Phenom Macrocycl Chem (2011) 71:381–388
DOI 10.1007/s10847-011-0016-5

ORIGINAL ARTICLE

Structural diversity in coordination polymers constructed from a naphthalene-spaced dipyridyl ligand and iron(II) thiocyanate

Feng Li · Jack K. Clegg · Cameron J. Kepert

Received: 28 April 2011 / Accepted: 13 July 2011 / Published online: 5 August 2011

Abstract Employing *N*,*N*′-bis-(4-pyridinylmethylene)-1,5-naphthalenediamine (nbpy4) and iron(II) thiocyanate as building blocks, three coordination polymers, $[Fe(NCS)_2(nbpy4)(MeOH)_2]_n$, **1**, $[Fe(NCS)_2(nbpy4)_2]_n \cdot 2nCHCl_3 \cdot nH_2O \cdot 2nEtOH$, **2**, and $[Fe(NCS)_2(nbpy4)(bpy)]_n \cdot 2.5nDCM \cdot 0.75nH_2O$, **3**, have been prepared. The three metal–organic materials were prepared by varying the solvent systems used and the inclusion of a second pyridine containing ligand (4,4′-bipyridine, bpy). Single crystal X-ray diffraction revealed **1** to be a one-dimensional structure with hydrogen bonding between adjacent chains and **2–3** to be two-dimension network solids with (4,4)-topologies.

Keywords Iron(II) · Dipyridyl · MOF · Coordination polymer · XRD

Introduction

Coordination polymers, also known as metal–organic framework materials, have received very considerable attention [1–6], due to their potential applications in catalysis [7–9], magnetism [10–17], gas adsorption [18–23], and non-linear optical and photoactive properties [24–26]. The choice of suitable organic components and appropriate metal ions plays important roles in the construction such assemblies, but the rational design and synthesis of polymeric coordination nets with particular degrees of interpenetration, dimensionality and framework connectivity still remains a significant challenge. To better understand the subtleties of various effects including solvent choice, systematic studies are required. Polypyridyl ligands, which contain two or more pyridyl groups separated by various linkers, have proven to be excellent building blocks for numerous supramolecular architectures [5, 27–34]. In previous studies we have investigated the synthesis of a series of metal–organic frameworks with different polymeric dimensionality and complexity employing dipyridyl ligands as the organic components for host–guest and spin-crossover studies [5, 13, 29, 35–47]. The results illustrate a temperature-dependent spin equilibrium between low-spin and high-spin states and guest-induced spin-crossover environments. It is clear from both our studies as well as those of others that bis-pyridyl derivative of the above type show uncommon utility as structural elements for the construction of interesting discrete and extended metal–organic architectures. This paper presents three coordination polymers formed from iron(II)thiocyanate and *N*,*N*′-bis-(4-pyridinylmethylene)-1,5-naphthalenediamine (nbpy4, Fig. 1) units under various solvent and competing ligand conditions; nbpy4 can be considered as an expanded 4,4′-bipyridine in which the N···N distance has increased from ~7.1 to ~16 Å (Fig. 1).

This work is dedicated to Professor Len Lindoy on the occasion of his 75th birthday.

F. Li · J. K. Clegg · C. J. Kepert (✉)
School of Chemistry, The University of Sydney, Sydney, NSW 2006, Australia
e-mail: c.kepert@chem.usyd.edu.au

J. K. Clegg
Department of Chemistry, The University of Cambridge, Lensfield Rd, Cambridge CB2 1EW, UK

Experimental procedure

Materials and procedures

The reagents were obtained from commercial suppliers and used without further purification unless noted otherwise.

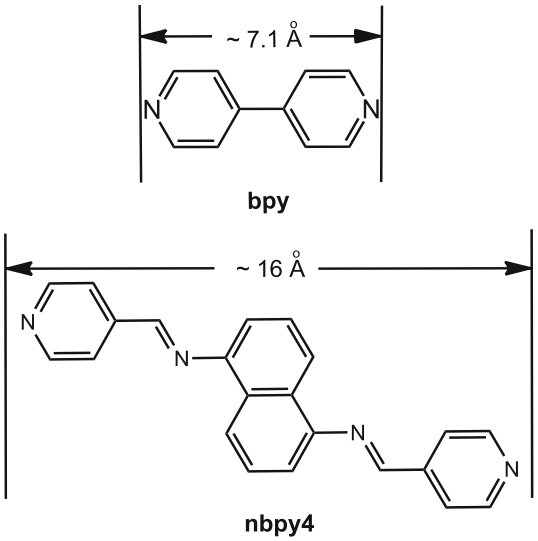

Fig. 1 Structures of bpy and nbpy4 with N···N separations

N ,*N*′-bis-(4-pyridinylmethylene)-1,5-naphthalenediamine, nbpy4, was prepared following the literature procedure, from 1,5-naphthalenediamine and pyridine-4-carboxaldehyde precursors [48–54]. UV–Vis spectra were measured using a Cary 5E Spectrophotometer equipped with an Omni-Diff™ diffuse reflectance probe. IR spectra were recorded on a Varian 800 Fourier transform infrared spectrometer (KBr). Elemental analyses for C, H and N were performed by Campbell Microanalytical Laboratory, University of Otago.

Framework synthesis

$[Fe(NCS)_2(nbpy4)(MeOH)_2]_n$ (**1**): A solution of $Fe(ClO_4)_2 \cdot 6H_2O$ (13.5 mg, 0.0372 mmol) in methanol (10 mL) was laid onto a mixture solution of nbpy4 ligand (25 mg, 0.0743 mmol) and NH_4SCN (5.7 mg, 0.0743 mmol) in $CH_3OH/CHCl_3$ (v:v = 1:5, 25 mL) in a test tube. The solution was left for 3 weeks at room temperature to give X-ray quality red block crystal. After filtration, the product was washed with CH_3OH and then allowed to stand in air prior to analysis. Yield: ≈72%. UV–Vis (solid state): 526 (sh), 454 (sh), 356 nm; IR (cm^{-1}, KBr): 3365(br), 3041(w), 2053(s), 1609(m), 1417(m), 823(m), 794(s); elemental analysis (%) calcd. for $C_{26}H_{24}FeN_6O_2S_2$: C 54.55, H 4.23, N 14.68; Found: C 54.88, H 4.63, N 14.91.

$[Fe(NCS)_2(nbpy4)_2]_n \cdot 2nCHCl_3 \cdot nH_2O \cdot 2nEtOH$ (**2**): A solution of $Fe(ClO_4)_2 \cdot 6H_2O$ (13.5 mg, 0.0372 mmol) in ethanol (10 mL) was layered onto a mixture solution of nbpy4 ligand (25 mg, 0.0743 mol) and NH_4SCN (5.7 mg, 0.0743 mmol) in $EtOH/CHCl_3$ (v:v = 1:5, 25 mL) in a test tube. The solution was left for a week at room temperature to give X-ray quality dark red block crystal. After filtration, the product was washed with EtOH and then allowed to stand in air prior to analysis. Yield: ≈81%. UV–Vis (solid state): 542 (sh), 360 nm; IR (cm^{-1}, KBr): 3394(br), 3034(w), 2051(s), 1609(m), 1417(m), 824(m), 794(s); elemental analysis (%) calcd. for $C_{46}H_{32}FeN_{10}S_2 \cdot 0.75CHCl_3$: C 60.10, H 3.53, N 14.99; Found: C 60.00, H 3.56, N 14.84.

$[Fe(NCS)_2(nbpy4)(bpy)]_n \cdot 2.5nDCM \cdot 0.75nH_2O$ (**3**): A solution of $Fe(ClO_4)_2 \cdot 6H_2O$ (16.2 mg, 0.0446 mmol) in ethanol (10 mL) was layered onto a mixture solution of nbpy4 (15 mg, 0.0446 mmol) and 4-4′-bipyridine ligands (7 mg, 0.0446 mmol) and NH_4SCN (6.8 mg, 0.0892 mmol) in EtOH/DCM (v:v = 1:5, 25 mL) in a test tube. The solution was left for a week at room temperature to give X-ray quality dark red block crystal. After filtration, the product was washed with EtOH and then allowed to stand in air prior to analysis. Yield: ≈88%. UV–Vis (solid state): 518 (sh), 424 nm; IR (cm^{-1}, KBr): 3450(br), 3048(w), 2061(s), 1608(m), 1407(m), 798(m); elemental analysis (%) calcd. for $C_{34}H_{24}FeN_8S_2 \cdot 0.75H_2O$: C 60.22, H 3.79, N 16.52; Found: C 60.11, H 3.74, N 16.11.

X-ray structure determinations

Structural data for **1** and **3** were collected on a Bruker–Nonius APEXII-X8-FR591 diffractometer employing graphite-monochromated Mo-Kα radiation generated from a rotating anode (0.71073 Å) with ω and ψ scans [55]. Data for **2** were collected on a Bruker SMART 1000 diffractometer employing graphite-monochromated Mo-Kα radiation generated from a sealed tube (0.71073 Å) with ω scans [56]. All data were collected to approximately 56° 2θ. Data integration and reduction were undertaken with SAINT and XPREP [55, 56] and subsequent computations were carried out using the WinGX-32 graphical user interface [57]. Structures were solved by direct methods using SIR97 [58]. Multi-scan empirical absorption corrections were applied to data sets using the program SADABS [59]. Data were refined and extended with SHELXL-97 [60, 61]. In general, non-hydrogen atoms with occupancies greater than 0.5 were refined anisotropically. Carbon-bound hydrogen atoms were included in idealised positions and refined using a riding model, oxygen-bound hydrogen atoms were located in the difference Fourier map before refinement. Crystal data and specific refinement details are reported below.

1, *[Fe(NCS)$_2$(nbpy4)(MeOH)$_2$]$_n$*

Formula $C_{26}H_{24}FeN_6O_2S_2$, *M* 572.50, triclinic, space group *P* $\bar{1}$(#2), *a* 8.2267(2), *b* 8.25010(10), *c* 10.7397(2) Å, α 96.6174(8), *β* 110.8214(9), *γ* 94.1867(9)°, *V* 671.65(2) $Å^3$, D_c 1.415 g cm^{-3}, *Z* 1, crystal size 0.221 by 0.114 by 0.099 mm, colour orange, habit block, temperature

100(2) K, λ(MoKα) 0.71073 Å, μ(MoKα) 0.752 mm^{-1}, T(SADABS)$_{min,max}$ 0.6821, 0.7457, 2θ_{max} 56.62, *hkl* range −10 10, −11 10, −12 14, N 11186, N_{ind} 3301(R_{merge} 0.0208), N_{obs} 2807(I > 2σ(I)), N_{var} 191, residuals* $R1(F)$ 0.0763, $wR2(F^2)$ 0.1930, GoF(all) 1.054, $\Delta\rho_{min,max}$ −1.711, 1.594 e$^-$ Å^{-3}.

*$R1 = \Sigma^{||}F_o^{|} - {}^{|}F_c^{||}/\Sigma^{|}F_o^{|}$ for $F_o > 2\sigma(F_o)$; $wR2 = (\Sigma w(F_o^2 - F_c^2)^2/\Sigma(wF_c^2)^2)^{1/2}$ all reflections $w = 1/[\sigma^2(F_o^2) + (0.0682\,P)^2 + 2.5444P]$ where $P = (F_o^2 + 2F_c^2)/3$.

Specific details: The pyridyl components of the structure is disordered over two positions with 0.75 and 0.25 occupancy as is the methyl group of the coordinated methanol.

2, [Fe(NCS)$_2$(nbpy4)$_2$]$_n$·2nCHCl$_3$·nH$_2$O·2nEtOH

Formula $C_{52}H_{48}C_{l6}FeN_{10}O_3S_2$, M 1193.67, monoclinic, space group $C2/c$(#15), a 18.203(3), b 20.285(4), c 15.757(3) Å, β 95.694(3), V 5789.1(19) Å^3, D_c 1.370 g cm^{-3}, Z 4, crystal size 0.245 by 0.171 by 0.156 mm, colour red, habit block, temperature 100(2) K, λ(MoKα) 0.71073 Å, μ(MoKα) 0.659 mm^{-1}, T(SADABS)$_{min,max}$ 0.6133, 0.7456, 2θ_{max} 55.24, *hkl* range −23 23, −26 26, −20 20, N 27424, N_{ind} 6617(R_{merge} 0.1631), N_{obs} 2624(I > 2σ(I)), N_{var} 352, residuals* $R1(F)$ 0.0861, $wR2(F^2)$ 0.2916, GoF(all) 0.947, $\Delta\rho_{min,max}$−0.836, 1.557 e$^-$ Å^{-3}.

Specific details: The water and ethanol solvate molecules were each modelled as 50% occupancy, with one of the ethanol molecules also disordered over a symmetry position. The water hydrogen atoms could not be located in the difference Fourier map and were not modelled.

3, [Fe(NCS)$_2$(nbpy4)(bpy)]$_n$·2.5nDCM·0.75nH$_2$O

Formula $C_{35.25}H_{28}Cl_{2.50}FeN_8O_{0.75}S_2$, M 784.25, triclinic, space group $P\ \bar{1}$(#2), a 11.6394(3), b 11.9491(4), c 14.5833(4) Å, α 88.4280(10), β 82.3070(10), γ 77.9530(10)°, V 1965.73(10) Å^3, D_c 1.325 g cm^{-3}, Z 2, crystal size 0.112 by 0.065 by 0.035 mm, colour orange, habit prism, temperature 150(2) K, λ(MoKα) 0.71073 Å, μ(MoKα) 0.697 mm^{-1}, T(SADABS)$_{min,max}$ 0.6569, 0.7449, 2θ_{max} 46.60, *hkl* range −12 12, −13 13, −16 16, N 19784, N_{ind} 5598(R_{merge} 0.0490), N_{obs} 4175(I > 2σ(I)), N_{var} 449, residuals* $R1(F)$ 0.0617, $wR2(F^2)$ 0.1815, GoF(all) 1.039, $\Delta\rho_{min,max}$ −0.623, 1.139 e$^-$ Å^{-3}.

Specific details: The crystals employed in this study were small, susceptible to rapid solvent loss and were weakly diffracting; reflections were only observed to ~0.85 Å resolution. The two dichloromethane solvent molecules are each disordered over two positions (with 0.5, 0.25 and 0.25, 0.25 occupancy, respectively). A number of bond length restraints were required to facilitate realistic modelling. The solvent water molecule was modelled as disordered over three equal (0.25) occupancy positions. The water hydrogen atoms could not be located in the difference Fourier map and were not modelled.

Results and discussion

Reaction of nbpy4 with iron(II) perchlorate (M/L = 1:2 molar ratio) in the presence of ammonium thiocyanate in a mixture of methanol and chloroform yielded **1**, [Fe(NCS)$_2$(nbpy4)(MeOH)$_2$]$_n$. If instead the same procedure was repeated with same molar ratio of metal to ligand in a mixture of ethanol and chloroform a different complex, **2**, [Fe(NCS)$_2$(nbpy4)$_2$]$_n$·2nCHCl$_3$·nH$_2$O·2nEtOH resulted. Employing both nbpy4 and bpy simultaneously in an ethanol/dichloromethane solvent mixture afforded the mixed ligand complex **3**, [Fe(NCS)$_2$(nbpy4)(bpy)]$_n$·2.5nDCM·0.75nH$_2$O. X-ray structural analysis revealed that **1**–**3** are coordination polymers with different degrees of complexity (Scheme 1).

The solid state UV–Vis spectra of the coordination polymers over the region 900–350 nm revealed relatively intense bands 356 (**1**), 360 (**2**), 424 (**3**) nm and shoulders 526 (**1**), 454 (**1**), 542 (**2**) and 518 (**3**) nm. The latter's are attributed to a metal-to-ligand (MLCT) (d–π*) transition which is characteristic of an Fe(II) centre which is coordinated to a pyridyl-based ligand such as nbpy4 [62, 63]. The IR spectra of the coordination polymers display absorption bands at 1,609 (**1**), 1,609 (**2**) and 1,608 cm^{-1} (**3**) assignable to the C=N bond, consistent with frequencies observed for Schiff bases [64]. In addition, all materials display peaks consistent with the presence of the C≡N bond in thiocyanate (2,053 (**1**), 2,051(**2**) and 2,061 cm^{-1} (**3**)) [65].

1 crystallises as orange block-like crystals in the centrosymmetric triclinic space group $P\ \bar{1}$. Each *trans* Fe(II) centre has an octahedral geometry with the equatorial positions occupied by two *trans* *N*-bonded thiocyanate ligands and two *trans* methanol solvent molecules. The axial positions are filled by a bridging nbpy4 ligands coordinated by its pyridyl moiety resulting in a 1D polymeric structure that propagates along the crystallographic b $\bar{c}$ diagonal Fig. 2.

Each of the 1D-polymeric chains is involved in a series of interactions with the adjacent chains. The coordinated methanol molecules act as hydrogen bond donors and the imine nitrogen atoms as hydrogen bond acceptors (O(1)–N(1)^i = 2.835(5); O(1)–H(1)–N(1)^i = 166.1°; ^{i} −x + 1, −y + 2, −z + 2). The comparatively electron-poor pyridyl rings undergo offset face-to-face π–π interactions with the comparatively electron-rich naphthalene rings indicated by carbon–carbon distances of 3.3–4.0 Å. Combined with

Scheme 1 Schematic representation of syntheses of the three polymeric compounds **1**, **2** and **3**

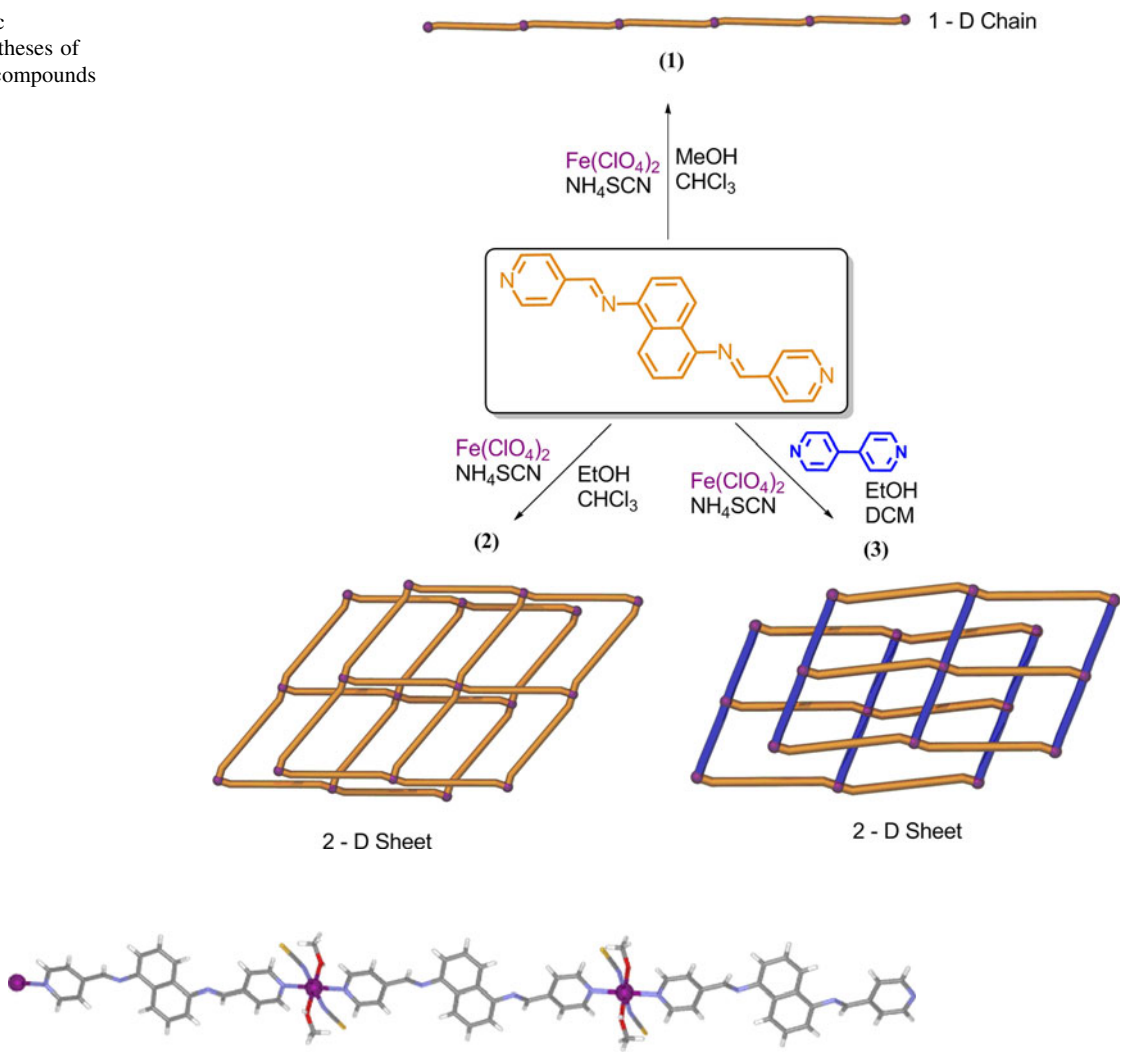

Fig. 2 Schematic representation of part of one of the 1D-polymeric chains in **1**. Selected bonds and angles: Fe(1)–$N_{thiocyanate}$ = 2.115(3); Fe(1)–O(1) = 2.148(4); Fe(1)–$N_{pyridyl}$ = 2.232(4); $N_{thiocyanate}$–Fe(1)–O(1) = 89.04(15); $N_{thiocyanate}$–Fe(1)–$N_{pyridyl}$ = 91.71(13); O(1)–Fe(1)–$N_{pyridyl}$ = 93.84(16)

the coordinate bonds these interactions result in the formation of infinite two-dimensional sheets that extend parallel to the crystallographic *bc*-plane (Fig. 3). Each of these two-dimensional sheets undergoes further weak (CH_{imine}–S = 2.86 Å) interactions with adjacent sheets forming a three-dimensional motif (Fig. 4).

2, $[Fe(NCS)_2(nbpy4)_2]_n \cdot 2nCHCl_3 \cdot nH_2O \cdot 2nEtOH$, crystallises as red block-like crystals in the monoclinic space group *C*2/*c*. In contrast to **1** the octahedral iron(II) centres have an N_6-coordination sphere with the *N*-bound thiocyanates occupying the axial positions and four bridging nbpy4 ligands occupying the equatorial positions (Fig. 5).

This coordination arrangement results in the formation of an infinite (4,4)-type [66] two-dimensional lattice that extends at nearly parallel to the crystallographic *bc*-plane (Fig. 6). Adjacent lattices pack slightly offset from each other interacting through weak edge-to-face (pyridyl-naphthalene CH–C = 2.9–3.2 Å) π–π interactions and weak $CH_{naphthalene}$–S (3.2–3.5 Å) hydrogen bonds. The slight offset results in the formation of small discrete pockets of void volume which are filled with the solvent molecules.

If 4,4′-bipyridine is also included in the reaction mixture a mixed ligand complex, **3**, $[Fe(NCS)_2(nbpy4)(bpy)]_n \cdot 2.5nDCM \cdot 0.75nH_2O$ resulted. **3** crystallises as small orange prismatic crystals in triclinic $P\,\overline{1}$. Once again the metal centres are octahedral with the ligands arranged in a *trans* configuration; four pyridyl donors (two bpy and two nbpy4) occupy the equatorial sites, while two *N*-coordinated thiocyanate ligands occupy the axial positions (Fig. 7).

The coordination geometry results in the formation of an infinite (4,4)-net [66] similar to that in **2**. The effect of the inclusion of the shorter bpy ligand as well as the nbpy4

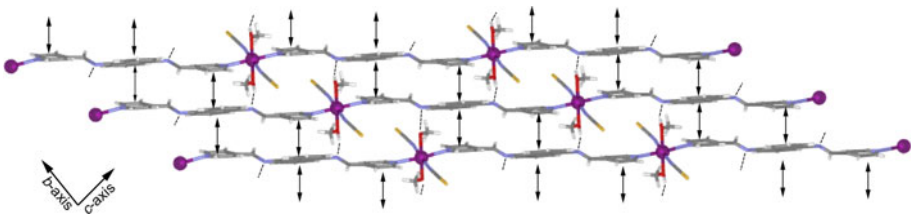

Fig. 3 Schematic representation of part of one of the 2D-sheets in **1**. *Dashed lines* indicate H-bonds, *double headed arrows* indicate π–π interactions

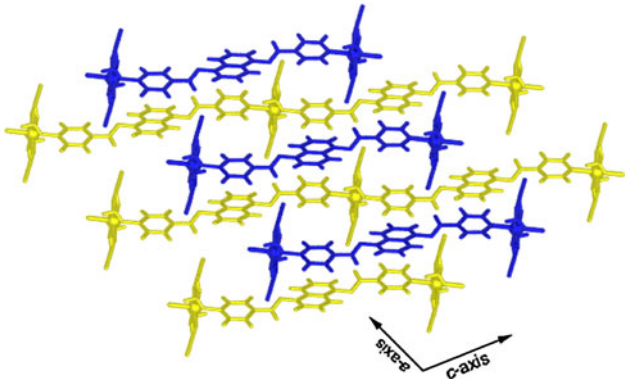

Fig. 4 Schematic representation of the 3D-arrangement in **1**. Adjacent 2D-sheets are coloured alternately

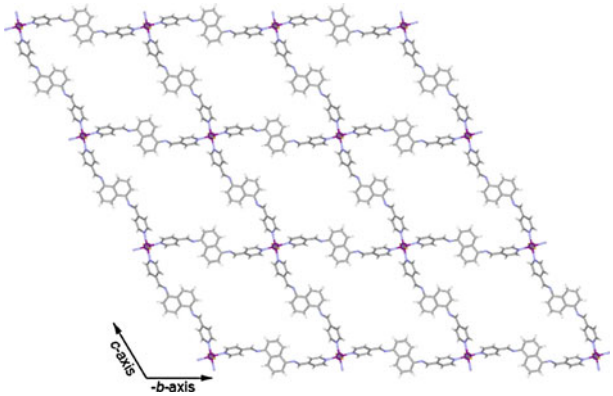

Fig. 6 Schematic representation of part of the infinite 2D lattice in **2**

ligands results in one side of the repeating parallelograms to be contracted compared to those in **2** (Fig. 8). Between adjacent layers are a number of edge-to-face π-π interactions between the bpy ligands and naphthalene groups (2.9–3.2 Å). The thiocyanate groups extend sufficiently far such that the sulfur atoms lie in the cavities of the adjacent layer, an arrangement stabilised by weak $CH_{napthalene}$–S hydrogen bonds. This packing arrangement leads to the formation of infinite solvent-filled channels that extend almost parallel to the crystallographic *c*-axis.

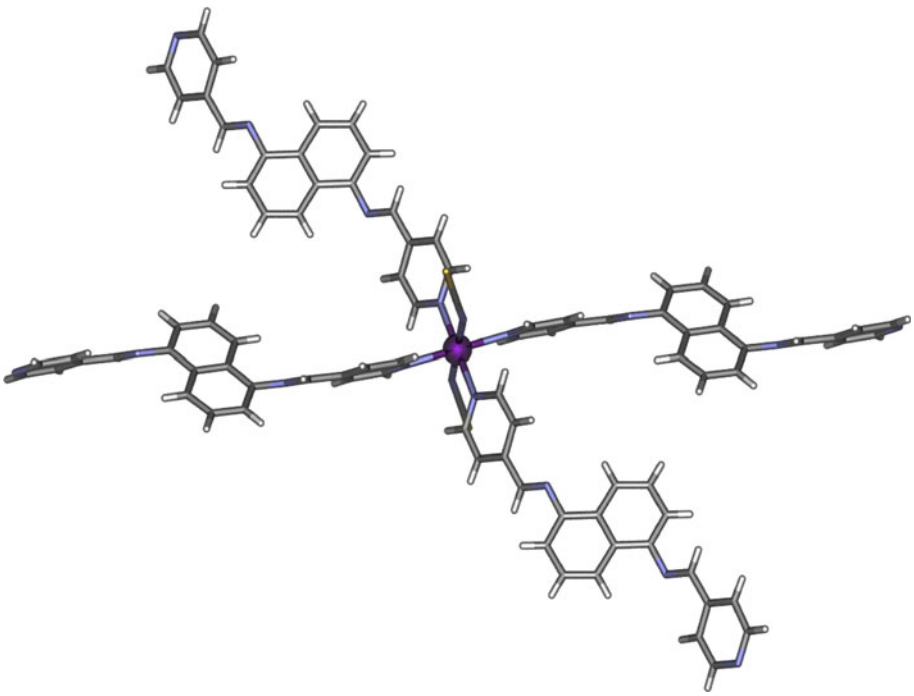

Fig. 5 Schematic representation of the coordination geometry in **2**. Selected bonds and angles: $Fe–N_{thiocyanate} = 2.081(6)$; $Fe(1)–N(1)_{pyridyl} = 2.221(5)$; $Fe(1)–N(4)_{pyridyl} = 2.233(5)$; $N_{thiocyanate}–Fe(1)–N(1)_{pyridyl} = 90.23(19)$; $N_{thiocyanate}–Fe(1)–N(4)_{pyridyl} = 90.7(2)$; $N(1)_{pyridyl}–Fe(1)–N(4)_{pyridyl} = 92.82(19)$

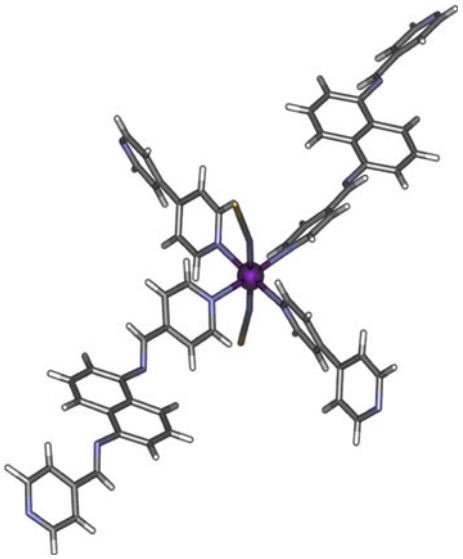

Fig. 7 Schematic representation of part of **3**. Selected bond lengths and angles: $Fe(1)–N(7)_{thiocyanate} = 2.080(4)$; $Fe(1)–N(8)_{thiocyanate}$ 2.103(5); $Fe(1)–N(3)_{nbpy4} = 2.204(4)$; $Fe(1)–N(2)_{nbpy4} = 2.231(4)$; $Fe(1)–N(6)_{bpy} = 2.253(4)$; $Fe(1)–N(5)_{bpy} = 2.273(4)$; $N(7)_{thiocyanate}–Fe(1)–N(3)_{nbpy4} = 90.25(16)$; $N(8)_{thiocyanate}–Fe(1)–N(3)_{nbpy4} = 91.33(16)$; $N(7)_{thiocyanate}–Fe(1)–N(2)_{nbpy4} = 90.36(16)$; $N(8)_{thiocyanate}–Fe(1)–N(2)_{nbpy4} = 87.98(16)$; $N(7)_{thiocyanate}–Fe(1)–N(6)_{bpy} = 92.85(15)$; $N(8)_{thiocyanate}–Fe(1)–N(6)_{bpy} = 88.87(15)$; $N(3)_{nbpy4}–Fe(1)–N(6)_{bpy} = 92.79(15)$; $N(2)_{nbpy4}–Fe(1)–N(6)_{bpy} = 90.02(14)$; $N(7)_{thiocyanate}–Fe(1)–N(5)_{bpy} = 90.69(15)$; $N(8)_{thiocyanate}–Fe(1)–N(5)_{bpy} = 87.59(15)$; $N(3)_{nbpy4}–Fe(1)–N(5)_{bpy} = 87.14(15)$; $N(2)_{nbpy4}–Fe(1)–N(5)_{bpy} = 90.00(15)$

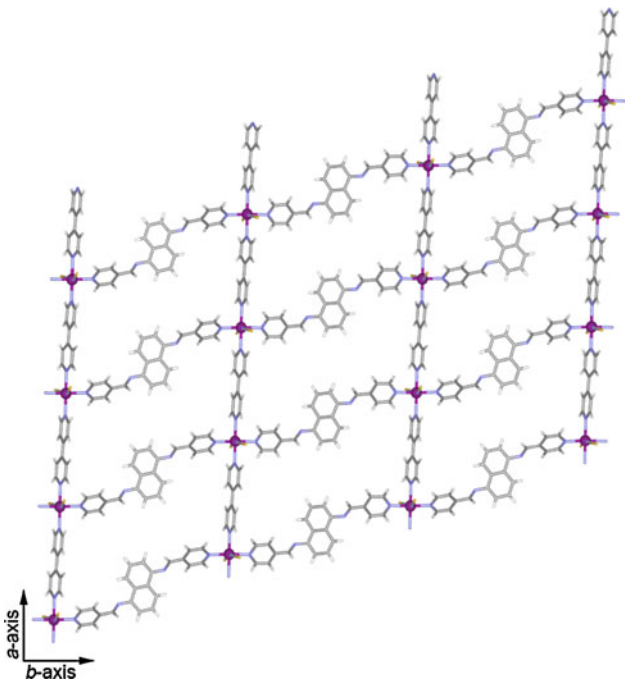

Fig. 8 Schematic representation of part of one of the two-dimensional sheets in **3**

Conclusions

In summary, we have demonstrated the diversity of polymeric architectures that can be formed from nbpy4 and $Fe(SCN)_2$ components by subtly controlling the synthetic conditions employed. Thus both 1D and 2D metal–organic coordination polymers based on this motif were prepared. Further investigations of the chemical and physical properties of materials formed from these subcomponents are ongoing.

Supplementary material

Crystallographic data for **1**, **2** and **3** have been deposited with CCDC, 12 Union Road, Cambridge CB2 1EZ, UK and are identified by deposition number CCDC 818255–818257. Copies of this information can be obtained free of charge on request by e-mail at deposit@ccdc.cam.ac.uk or at http://www.ccdc.cam.ac.uk

Acknowledgments We thank the Australian Research Council and J.K.C. acknowledges the Marie Curie IIF scheme of the 7th EU Framework Program for support. The authors thank Dr Deanna D'Alessandro for comments on UV–Vis Spectra.

References

1. Murray, L.J., Dinca, M., Long, J.R.: Hydrogen storage in metal-organic frameworks. Chem. Soc. Rev. **38**, 1294–1314 (2009)
2. Lee, J., Farha, O.K., Roberts, J., Scheidt, K.A., Nguyen, S.T., Hupp, J.T.: Metal-organic framework materials as catalysts. Chem. Soc. Rev. **38**, 1450–1459 (2009)
3. Perry IV, J.J., Perman, J.A., Zaworotko, M.J.: Design and synthesis of metal-organic frameworks using metal-organic polyhedra as supermolecular building blocks. Chem. Soc. Rev **38**, 1400–1417 (2009)
4. Tranchemontagne, D.J., Mendoza-Cortes, J.L., O'Keeffe, M., Yaghi, O.M.: Secondary building units, nets and bonding in the chemistry of metal-organic frameworks. Chem. Soc. Rev. **38**, 1257–1283 (2009)
5. Halder, G.J., Kepert, C.J., Moubaraki, B., Murray, K.S., Cashion, J.D.: Guest-dependent spin crossover in a nanoporous molecular framework material. Science **298**, 1762–1765 (2002)
6. Maspoch, D., Ruiz-Molina, D., Veciana, J.: Old materials with new tricks: multifunctional open-framework materials. Chem. Soc. Rev. **36**, 770–818 (2007)
7. Zou, R.-Q., Sakurai, H., Xu, Q.: Preparation, adsorption properties, and catalytic activity of 3D porous metal–organic frameworks composed of cubic building blocks and alkali-metal ions. Angew. Chem. Int. Ed. **118**, 2604–2608 (2006)
8. Ohara, K., Kawano, M., Inokuma, Y., Fujita, M.: A porous coordination network catalyzes an olefin isomerization reaction in the pore. J. Am. Chem. Soc. **132**, 30–31 (2009)
9. Kawamichi, T., Inokuma, Y., Kawano, M., Fujita, M.: Regioselecitive huisgen cycloaddition within porous coordination networks. Angew. Chem. Int. Ed. **49**, 2375–2377 (2010)
10. Coronado, E., Gatteschi, D.: Trends and challenges in molecule-based magnetic materials. J. Mater. Chem. **16**, 2513–2515 (2006)

11. Wang, D., Zhang, B., He, C., Wu, P., Duan, C.: A new chiral N-heterocyclic carbene silver(I) cylinder: synthesis, crystal structure and catalytic properties. Chem. Commun. **46**, 4728–4730 (2010)
12. Kepert, C.J.: Supramolecular magnetic materials. Aust. J. Chem. **62**, 1079–1080 (2009)
13. Neville, S.M., Halder, G.J., Chapman, K.W., Duriska, M.B., Moubaraki, B., Murray, K.S., Kepert, C.J.: Guest tunable structure and spin crossover properties in a nanoporous coordination framework material. J. Am. Chem. Soc. **131**, 12106–12108 (2009)
14. Southon, P.D., Liu, L., Fellows, E.A., Price, D.J., Halder, G.J., Chapman, K.W., Moubaraki, B., Murray, K.S., Letard, J.-F., Kepert, C.J.: Dynamic interplay between spin-crossover and host-guest function in a nanoporous metal–organic framework material. J. Am. Chem. Soc. **131**, 10998–11009 (2009)
15. Bechlars, B., D'Alessandro, D.M., Jenkins, D.M., Iavarone, A.T., Glover, S.D., Kubiak, C.P., Long, J.R.: High-spin ground states via electron delocalization in mixed-valence imidazolate-bridged divanadium complexes. Nat. Chem **2**, 362–368 (2010)
16. Sato, S., Morohara, O., Fujita, D., Yamaguchi, Y., Kato, K., Fujita, M.: Parallel-stacked aromatic hosts for orienting small molecules in a magnetic field: induced residual dipolar coupling by encapsulation. J. Am. Chem. Soc. **132**, 3670–3671 (2010)
17. Batten, S.R., Murray, K.S.: Structure and magnetism of coordination polymers containing dicyanamide and tricyanomethanide. Coord. Chem. Rev. **246**, 103–130 (2003)
18. Iremonger, S.S., Southon, P.D., Kepert, C.J.: A nanoporous chiral metal-organic framework material that exhibits reversible guest adsorption. Dalton Trans. **44**, 6103–6105 (2008)
19. Furukawa, H., Yaghi, O.M.: Storage of hydrogen, methane, and carbon dioxide in highly porous covalent organic frameworks for clean energy applications. J. Am. Chem. Soc. **131**, 8875–8883 (2009)
20. Britt, D., Furukawa, H., Wang, B., Glover, T.G., Yaghi, O.M.: Highly efficient separation of carbon dioxide by a metal-organic framework replete with open metal sites. Proc. Natl. Acad. Sci. USA **106**, 20637–20640 (2009)
21. Brown, C.M., Liu, Y., Yildirim, T., Peterson, V.K., Kepert, C.J.: Hydrogen adsorption in HKUST-1: a combined inelastic neutron scattering and first-principles study. Nanotechnology **20**, 204025 (2009)
22. Duriska, M.B., Neville, S.M., Lu, J., Iremonger, S.S., Boas, J.F., Kepert, C.J., Batten, S.R.: Systematic Metal Variation and Solvent and Hydrogen-Gas Storage in Supramolecular Nanoballs. Angew. Chem., Int. Ed. **48**, 8919–8922 (2009)
23. Clegg, J.K., Iremonger, S.S., Hayter, M.J., Southon, P.D., MacQuart, R.B., Duriska, M.B., Jensen, P., Turner, P., Jolliffe, K.A., Kepert, C.J., Meehan, G.V., Lindoy, L.F.: Hierarchical self-assembly of a chiral metal–organic framework displaying pronounced porosity. Angew. Chem. Int. Ed. **49**, 1075–1078 (2010)
24. Janiak, C.: Engineering coordination polymers towards applications. Dalton. Trans. **14**, 2781–2804 (2003)
25. Bünzli, J.-C.G., Piguet, C.: Lanthanide-containing molecular and supramolecular polymetallic functional assemblies. Chem. Rev. **102**, 1897–1928 (2002)
26. de Sá, G.F., Malta, O.L., de Mello Donegá, C., Simas, A.M., Longo, R.L., Santa-Cruz, P.A., da Silva, E.F.: Spectroscopic properties and design of highly luminescent lanthanide coordination complexes. Coord. Chem. Rev. **196**, 165–195 (2000)
27. Gass, I.A., Batten, S.R., Forsyth, C.M., Moubaraki, B., Schneider, C.J., Murray, K.S.: Supramolecular aspects of iron(II) crown-dipyridyl spin-crossover compounds. Coord. Chem. Rev. **255**, 2058–2067 (2011)
28. Glasson, C.R.K., Lindoy, L.F., Meehan, G.V.: Recent developments in the d-block metallo-supramolecular chemistry of polypyridyls. Coord. Chem. Rev. **252**, 940–963 (2008)
29. Halder, G.J., Kepert, C.J.: Iron(II) molecular framework materials with 4, 4'-azopyridine. Aust. J. Chem. **58**, 311–314 (2005)
30. Schilter, D., Clegg, J.K., Harding, M.M., Rendina, L.M.: Platinum(II) and palladium(II) metallomacrocycles derived from cationic 4, 4'-bipyridinium, 3-aminopyrazinium and 2-aminopyrimidinium ligands. Dalton Trans. **39**, 239–247 (2010)
31. Glasson, C.R.K., Clegg, J.K., McMurtrie, J.C., Meehan, G.V., Lindoy, L.F., Motti, C.A., Moubaraki, B., Murray, K.S., Cashion, J.D.: Unprecedented encapsulation of a $[Fe^{III}Cl_4]^-$ anion in a cationic $[Fe^{II}{}_4L_6]^{8+}$ tetrahedral cage derived from 5, 5‴-dimethyl-2, 2′:5′, 5″:2″, 2‴-quaterpyridine. Chem. Sci. **2**, 540–543 (2011)
32. Glasson, C.R.K., Meehan, G.V., Clegg, J.K., Lindoy, L.F., Turner, P., Duriska, M.B., Willis, R.: A new Fe^{II} quaterpyridyl M_4L_6 tetrahedron exhibiting selective anion binding. Chem. Commun. **10**, 1190–1192 (2008)
33. Glasson, C.R.K., Meehan, G.V., Clegg, J.K., Lindoy, L.F., Smith, J.A., Keene, F.R., Motti, C.: Microwave synthesis of a rare $[Ru_2L_3]^{4+}$ triple helicate and its interaction with DNA. Chem. Eur. J. **14**, 10535–10538 (2008)
34. Hristova, Y.R., Smulders, M.M.J., Clegg, J.K., Breiner, B., Nitschke, J.R.: Selective anion binding by a "Chameleon" capsule with a dynamically reconfigurable exterior. Chem. Sci. **2**, 638–641 (2011)
35. Neville, S.M., Leita, B.A., Halder, G.J., Kepert, C.J., Moubaraki, B., Letard, J.-F., Murray, K.S.: Understanding the two-step spin-transition phenomenon in iron(II) 1D chain materials. Chem. Eur. J. **14**, 10123–10133 (2008)
36. Neville, S.M., Halder, G.J., Chapman, K.W., Duriska, M.B., Southon, P.D., Cashion, J.D., Letard, J.-F., Moubaraki, B., Murray, K.S., Kepert, C.J.: Single-crystal to single-crystal structural transformation and photomagnetic properties of a porous iron(ii) spin-crossover framework. J. Am. Chem. Soc. **130**, 2869–2876 (2008)
37. Mulyana, Y., Kepert, C.J., Lindoy, L.F., McMurtrie, J.C.: New cadmium(II) and iron(II) coordination frameworks incorporating a Di(4-pyridyl)isoindoline ligand. Eur. J. Inorg. Chem. **12**, 2470–2475 (2005)
38. Halder, G.J., Kepert, C.J.: In situ single-crystal X-ray diffraction studies of desorption and sorption in a flexible nanoporous molecular framework material. J. Am. Chem. Soc. **127**, 7891–7900 (2005)
39. Halder, G.J., Chapman, K.W., Neville, S.M., Moubaraki, B., Murray, K.S., Letard, J.-F., Kepert, C.J.: Elucidating the mechanism of a two-step spin transition in a nanoporous metal–organic framework. J. Am. Chem. Soc. **130**, 17552–17562 (2008)
40. Cussen, E.J., Claridge, J.B., Rosseinsky, M.J., Kepert, C.J.: Flexible sorption and transformation behavior in a microporous metal–organic framework. J. Am. Chem. Soc. **124**, 9574–9581 (2002)
41. Fletcher, A.J., Cussen, E.J., Prior, T.J., Rosseinsky, M.J., Kepert, C.J., Thomas, K.M.: Adsorption dynamics of gases and vapors on the nanoporous metal organic framework material Ni_2(4, 4'-Bipyridine)3(NO_3)4: guest modification of host sorption behavior. J. Am. Chem. Soc. **123**, 10001–10011 (2001)
42. Beves, J.E., Constable, E.C., Housecroft, C.E., Kepert, C.J., Neuburger, M., Price, D.J., Schaffner, S.: The conjugate acid of bis{4'-(4-pyridyl)-2, 2′:6′, 2″-terpyridine}iron(II) as a self-complementary hydrogen-bonded building block. Cryst. Eng. Comm. **9**, 1073–1077 (2007)
43. Beves, J.E., Bray, D.J., Clegg, J.K., Constable, E.C., Housecroft, C.E., Jolliffe, K.A., Kepert, C.J., Lindoy, L.F., Neuburger, M., Price, D.J., Schaffner, S., Schaper, F.: Expanding the 4, 4′-bipyridine ligand: Structural variation in $\{M(pytpy)2\}^{2+}$ complexes (pytpy = 4'-(4-pyridyl)-2, 2′:6′, 2″-terpyridine, M = Fe, Ni, Ru) and assembly of the hydrogen-bonded, one-dimensional polymer $\{[Ru(pytpy)(Hpytpy)]\}_n^{3n+}$. Inorg. Chim. Acta. **361**, 2582–2590 (2008)

44. Beves, J.E., Dunphy, E.L., Constable, E.C., Housecroft, C.E., Kepert, C.J., Neuburger, M., Price, D.J., Schaffner, S.: Vectorial property dependence in bis{4'-(n-pyridyl)-2, 2′:6′, 2″-terpyridine}iron(II) and ruthenium(II) complexes with n = 2, 3 and 4. Dalton. Trans. **3**, 386–396 (2008)
45. Beves, J.E., Constable, E.C., Housecroft, C.E., Kepert, C.J., Price, D.J.: The first example of a coordination polymer from the expanded 4, 4'-bipyridine ligand [Ru(pytpy)2]2 + (pytpy = 4'-(4-pyridyl)-2, 2′:6′, 2″-terpyridine). Cryst. Eng. Comm. **9**, 456–459 (2007)
46. Amoore, J.J.M., Neville, S.M., Moubaraki, B., Iremonger, S.S., Murray, K.S., Letard, J.-F., Kepert, C.J.: Thermal- and light-induced spin crossover in a guest-dependent dinuclear iron(II) system. Chem. Eur. J. **16**, 1973–1982 (2010)
47. Amoore, J.J.M., Kepert, C.J., Cashion, J.D., Moubaraki, B., Neville, S.M., Murray, K.S.: Structural and magnetic resolution of a two-step full spin-crossover transition in a dinuclear iron(II) pyridyl-bridged compound. Chem. Eur. J. **12**, 8220–8227 (2006)
48. Su, C.-Y., Goforth, A.M., Smith, M.D., zur Loye, H.-C.: Assembly of large simple 1D and rare polycatenated 3D molecular ladders from T-shaped building blocks containing a new, long *N*, *N*′-bidentate ligand. Chem. Commun. **19**, 2158–2159 (2004)
49. Liu, Y.-R., Li, X.-P., Zhang, J.-A., Su, C.-Y.: *N*, *N*′-Bis(4-pyridylmethylene)naphthalene-1, 5-diamine. Acta. Cryst. **61**, o2089–o2090 (2005)
50. Jang, Y.O., Lee, S.W.: Homoleptic silver-bis(pyridine) coordination polymers: $[Ag(L^1)_2]$ (PF_6), $[Ag(L^1)_2]$ (SbF_6), $[Ag(L^1)_2]$ (BF_4), $[Ag(L^2)]$ (PF_6), and $[Ag(L^3)_{1.5}]$ (CF_3SO_3) $(H_2O)_2$ {L^1 = (4-py)-CH=N–$C_{10}H_6$–N=CH–(4-py); L^2 = (2-py)–CH=N–$C_{10}H_6$–N=CH–(2-py); L^3 = (3-py)–CH=N–$C_{14}H_{12}$–N=CH–(3-py)}. Polyhedron **29**, 2731–2738 (2010)
51. Jung, Y.-M., Lee, S.W.: Relative coordinating abilities of bis(pyridine)-type ligands when forming mixed-ligand coordination polymers: preparation and structure of $[Cd_2(L^1)_2(L^2)(NO_3)_4]$.infin. {(*n*-py)-CH=N–$C_{10}H_6$–N=CH–(*n*-py) [*n* = 3 (L^1), 4 (L^2)]}. Bull. Korean Chem. Soc. **31**, 2668–2671 (2010)
52. Min, D., Cho, B.-Y., Lee, S.W.: Novel long bipyridine-type linking ligands containing an intervening naphthalene fragment: $[Zn(L^1)(NO_3)_2]$, $[Zn(L^2)(NO_3)_2]$, and $[Cd(L^1)_{1.5}(NO_3)_2]$ (L^1 = (4-py)–CHN–$C_{10}H_6$–NCH–(4-py); L^2 = (3-py)–CHN–$C_{10}H_6$–NCH–(3-py)). Inorg. Chim. Acta. **359**, 577–584 (2006)
53. Kim, S.H., Huh, H.S., Lee, S.W.: Cobalt(II) coordination polymers based on dicarboxylates and dipyridyl-type ligands: $[CoL_{1.5}(NO_3)_2]$, $[Co_{1.5}(bpdc)_{1.5}(dma)$ (dma) (EtOH), $[Co_{1.5}(ndc)_{1.5}(dma)_2]$, $[Co_3(ndc)_3(dmf)_4]$, and [CoL(bpdc)] (EtOH) ($bpdcH_2$ = biphenyl-4, 4'-dicarboxylic acid, $ndcH_2$ = 2, 6-naphthalene dicarboxylic acid, L = pyCH=N–C10H6–N=CHpy). J. Mol. Struct. **841**, 78–87 (2007)
54. Huh, H.S., Lee, S.W.: {μ-*N*,*N*'-Bis[(E)-4-pyridylmethylidene] naphthalene-1,5-diamine}bis[dichlorido(dimethyl sulfide)platinum (II)]. Acta. Cryst. **E64**, m1138 (2008)
55. Bruker-Nonius: APEX v2.1, SAINT v.7 and XPREP v.6.14. Bruker AXS Inc., Madison (2003)
56. Bruker: SMART, SAINT and XPREP. Bruker Analytical X-ray Instruments Inc., Wisconsin (1995)
57. Farrugia, L.J.: WinGX suite for small-molecule single-crystal crystallography. J. Appl. Cryst. **32**, 837–838 (1999)
58. Altomare, A., Burla, M.C., Camalli, M., Cascarano, G.L., Giocavazzo, C., Gaugliardi, A., Moliterni, G.C., Polidori, G., Spagna, S.: SIR97, A package for crystal structure solution by direct methods and refinement. J. Appl. Cryst. **32**, 115–119 (1999)
59. Sheldrick, G.M.: SADABS. Empirical absorption and correction software. University of Göttingen, Germany (1996–2008)
60. Sheldrick, G.M.: A short history of *SHELX*. Acta. Cryst. A **64**, 112–122 (2008)
61. Sheldrick, G.M.: SHELXL-97: programs for crystal structure analysis. University of Göttingen, Germany (1997)
62. Xia, H.-L., Ardo, S., Narducci Sarjeant, A.A., Huang, S., Meyer, G.J.: Photodriven spin change of Fe(II) benzimidazole compounds anchored to nanocrystalline TiO_2 thin films. Langmuir **25**, 13641–13652 (2009)
63. Létard, J.F., Nguyen, O., Soyer, H., Mingotaud, C., Delhaès, P., Kahn, O.: First evidence of the LIESST effect in a Langmuir–Blodgett film. Inorg. Chem. **38**, 3020–3021 (1999)
64. Vigato, P.A., Tamburini, S.: The challenge of cyclic and acyclic schiff bases and related derivatives. Coord. Chem. Rev. **248**, 1717–2128 (2004)
65. Capitán-Vallvey, L.F., Jimenez, C.: Spectrophotometric extractive determination of thiocyanate as a mixed-ligand iron-thiocyanate-2-(phenyliminomethyl)pyridine complex. Microchem. J. **28**, 118–125 (1983)
66. Wells, A.F.: Three-dimensional nets and polyhedra. Wiley-Interscience, New York (1977)